

A Dosimetry Model for the Small Intestine Incorporating Intestinal Wall Activity and Cross-Doses

Lena Jönsson, MSc¹; Xiaowei Liu, PhD²; Bo-Anders Jönsson, PhD¹; Michael Ljungberg, PhD¹; and Sven-Erik Strand, PhD¹

¹Department of Radiation Physics, The Jubileum Institute, Lund University, Lund University Hospital, Lund, Sweden; and ²Department of Physics, Zhongshan University, Guangzhou, China

Current internal radiation dosimetry models for the small intestine, and for most walled organs, lack the ability to account for the activity uptake in the intestinal wall. In existing models the cross-dose from nearby loops of the small intestine is not taken into consideration. The aim of this investigation was to develop a general model for calculating the absorbed dose to the radiation-sensitive cells in the small intestinal mucosa from radionuclides located in the small intestinal wall or contents. **Methods:** A model was developed for calculation of the self-dose and cross-dose from activity in the intestinal wall or contents. The small intestine was modeled as a cylinder with 2 different wall thicknesses and with an infinite length. Calculations were performed for various mucus thicknesses. S values were calculated using the EGS4 Monte Carlo simulation package with the PRESTA algorithm and the simulation results were integrated over the depth of the radiosensitive cells. The cross-organ dose was calculated by summing the dose contributions from other intestinal segments. Calculations of S values for self-dose and cross-dose were made for monoenergetic electrons, 0.050–10 MeV, and for the radionuclides ^{99m}Tc, ¹¹¹In, ¹³¹I, ⁶⁷Ga, ⁹⁰Y, and ²¹¹At. **Results:** The self-dose S value from activity located in the small intestinal wall is considerably greater than the S values for self-dose from the contents and the cross-dose from wall and contents except for high electron energies. For all radionuclides investigated and for electrons 0.10–0.20 MeV and 8–10 MeV in energy, the cross-dose from activity in the contents is higher than the self-dose from the contents. The mucus thickness affects the S value when the activity is located in the contents. **Conclusion:** A dosimetric model for the small intestine was developed that takes into consideration the localization of the radiopharmaceutical in the intestinal wall or in the contents. It also calculates the contribution from self-dose and cross-dose. With this model, more accurate calculations of absorbed dose to radiation-sensitive cells in the intestine are possible.

Key Words: radiation dosimetry; intestine; cross-dose; EGS4; Monte Carlo simulations

J Nucl Med 2002; 43:1657–1664

Received Jul. 9, 2001; revision accepted Apr. 25, 2002.
For correspondence or reprints contact: Lena Jönsson, MSc, Department of Radiation Physics, Lund University Hospital, SE-221 85 Lund, Sweden.
E-mail: Lena.Jonsson@radfys.lu.se

Radiopharmaceuticals might be partially excreted from the body through the intestinal tract or localized in the intestinal wall. An accurate intestinal dosimetry model should be able to calculate the absorbed dose to the radiation-sensitive crypt cells in the small intestinal wall. Accurate dosimetry calculations are especially important when high activities are administered to the patient and a significant fraction of the radionuclide is excreted through the intestinal tract. From a dosimetric point of view, it is important to know the activity distribution in the intestinal wall. However, it is impossible to distinguish between activity localized in the intestinal contents and activity uptake in the small intestinal wall in nuclear medicine imaging. Many internal dosimetry models therefore simply assume that the radiopharmaceutical is located in the intestinal contents (1–4). Through complementary experimental animal studies, the activity distribution in the intestinal wall and in the contents can be revealed by dissecting the animals, measuring the tissue radioactivity uptake, and performing autoradiography of the excised organs.

In a previous autoradiographic study in rats by our group (5), the biodistribution of different ¹¹¹In-labeled radiopharmaceuticals showed an activity uptake in the small intestinal wall. Other studies on ²⁰¹Tl- and ²⁰⁴Tl-labeled radiopharmaceuticals (6,7) also revealed that 15%–19% of the activity was localized in the small intestinal wall in mice.

The mean absorbed dose to an organ is calculated using the general method developed by the MIRD Committee (8). A key parameter in the MIRD concept is the $S(r_k \leftarrow r_h)$ value, defined as the mean absorbed dose to the target region r_k , per unit cumulated activity in the source region r_h . The mean absorbed dose to the target region r_k from the source region r_h , $\bar{D}(r_k \leftarrow r_h)$, is then calculated from:

$$\bar{D}(r_k \leftarrow r_h) = \tilde{A}(r_h) \cdot S(r_k \leftarrow r_h), \quad \text{Eq. 1}$$

where $\tilde{A}(r_h)$ is the cumulated activity in the source region r_h .

The model used for calculation of the absorbed dose to the small intestine, given in MIRD Pamphlet No. 11 (2),

TABLE 1
Data for Various Small Intestinal Dosimetry Models

Reference	Small intestinal model	Small intestinal radius (mm)	Small intestinal wall thickness (mm)	Villi height (μm)	Crypt depth (μm)	Mucus thickness (μm)
ICRP (1,9)	Cylinder/region*	10	2-3	500-1,500	20-450	—
MIRD (10)	Cylinder/region*	—	3-4	—	—	—
Stubbs et al. (3)	Cylinder	10	5	500	150	200
Poston et al. (4)	Cylinder	12.46	7.54	—	300-600 [†]	—
This work	Cylinder/cross	12.5	3 and 6	500	150	5-200

*Cylinder for nonpenetrating radiation and model as large soft-tissue region with no delineation of content and wall regions, for penetrating radiation.

[†]Assumed target cell layer.

separates the intestinal wall and contents. For electrons it is assumed that the dose to the wall is half the dose to the contents far from the wall, when the activity is in the contents. The dose to the intestinal wall from sources in the contents represents a surface dose from electrons. The average dose for wall and contents is calculated for the photons.

In the model of the International Commission on Radiation Protection (ICRP) (1) the specific absorbed fraction is calculated for the mucosal layer of the intestine for nonpenetrating radiation (e.g., electrons). For penetrating radiation the small intestine is modeled as a large soft-tissue volume where the wall and the contents are not differentiated. The average absorbed dose to the wall and the contents represents the absorbed dose to the mucosal layer.

More detailed models of the small intestine have been presented by Stubbs et al. (3) and by Poston et al. (4). In the study of Stubbs et al. (3) the small intestine is modeled as 2 concentric cylinders, where the inner cylinder represents the intestinal contents and the volume between the 2 cylinders corresponds to the intestinal wall. Calculations of S values for various radionuclides were made as a function of distance from the contents-mucus interface.

Poston et al. (4) calculated the absorbed fraction for the part of the intestinal wall where the most sensitive cells are thought to be located. Data for the small intestinal models are summarized in Table 1.

The specific absorbed fraction with the small intestinal wall as the source organ is given in a study by Stabin et al. (11). Data are presented for several photon energies for pregnant and nonpregnant woman.

This study presents a refined model of the small intestine for calculation of the absorbed dose to the radiosensitive crypt cells from activity localized in the intestinal wall and including the contribution of the cross-dose from neighboring loops of intestine, factors not incorporated to date into dosimetric models of the small intestine. The investigation is based on uniformly distributed activity in the contents and in the intestinal wall. The S values for villi and for crypt cells were calculated for monoenergetic electrons and for several radionuclides. Simulations were made for wall thicknesses of 3 and 6 mm. The thickness of the small intestinal mucus layer is not well defined in the literature, and the influence of different thicknesses of the layer on the S value has thus also been investigated.

MATERIALS AND METHODS

Intestinal Model

The small intestine was simulated as 2 concentric cylinders (Fig. 1), where the inner cylinder corresponds to the small intestinal contents and has a diameter of 25 mm. The volume between the inner and the outer cylinder represents the small intestinal wall.

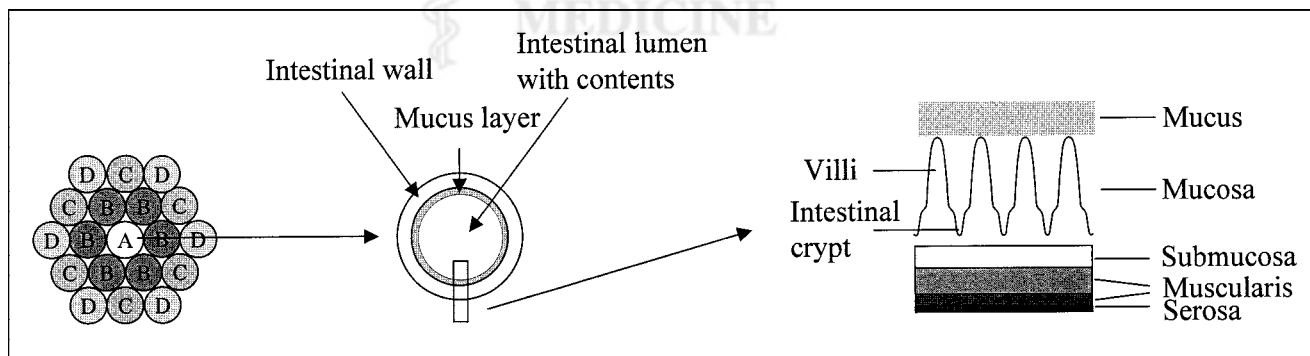


FIGURE 1. Geometry used in small intestinal wall model. (Left) Geometry of intestinal loops used to calculate cross-dose to segment A from closest (B), next closest (C), and third closest (D) segments. (Center) Enlarged cross-section of small intestinal model. (Right) Schematic illustration of intestinal wall anatomy, with location of villi and crypt cells.

Two intestinal wall thicknesses (3 and 6 mm) were chosen for the calculations. Concentric ranges of wall thicknesses were assigned to the villi (500 μm) and to the crypt cells (150 μm). Few data on the mucus thickness in the small bowel are given in the literature. Therefore, 4 values of mucus thickness—5, 50, 100, and 200 μm —were used in the calculations of the S values. A length of 3 m was used for the small intestine, corresponding to the in vivo length of a contracted intestine (this value will be about 6 m in a corpse) (12–15). The tissue was considered water equivalent.

The model was used for calculation of the self-dose from activity located in the contents and in the intestinal wall. The cross-dose from nearby loops of the small intestine was also simulated. Because of the complexity of the small intestinal geometry, a simplified model for the loops was derived on the basis of a hexagonal tube system (Fig. 1). In the calculation of the cross-dose, 20-cm segments of the intestine were hexagonally arranged and the dose contribution from all intestinal loops was calculated (Fig. 1).

Calculations of S Values and Absorbed Dose

The S values for the radiation-sensitive cells were calculated in 2 steps. First, the distribution of the energy imparted as a function of the distance from the contents–mucus interface was simulated using the EGS4 Monte Carlo package with the PRESTA algorithm (16). The S values were then calculated from the simulation results by integration of the energy imparted in the sensitive-cells region and division by the mass of the volume of interest. In the simulation, the length of the intestine was modeled as infinite, the electron and photon cutoff energies were set at 10-keV kinetic energy and 1 keV, respectively, and the fractional energy loss per step for electrons was set to 2%. The number of histories was set to keep the uncertainty <5% (SD for 10 independent runs), except for low electron energies (0.050–0.10 MeV), where the uncertainty was <10%.

The S values were calculated per centimeter of small intestine ($\mu\text{Gy cm MBq}^{-1} \text{s}^{-1}$). In this study, a length of 300 cm was used for the small intestine and so the presented S values ($\mu\text{Gy MBq}^{-1} \text{s}^{-1}$) are all divided by 300. The cumulated activity in the source region, $\tilde{A}(r_h)$, in Equation 1 should therefore be calculated for the total small intestine.

The cross-organ S values were calculated by summing the energy-imparted contributions from other intestine segments—that is, from the closest segments, the next closest segments, and the third closest segments. The cross-organ S value is largest when the segment is located at the center of the hexagon, and therefore all S values were calculated for segment A. The contributions from the closest segments $S_{A \leftarrow B}$, the next closest segments $S_{A \leftarrow C}$, and the third closest segments $S_{A \leftarrow D}$ were calculated by integration of the simulation results. The cross-organ S value for segment A (Fig. 1) was then calculated as $S_A = 6 \cdot (S_{A \leftarrow B} + S_{A \leftarrow C} + S_{A \leftarrow D})$ because of the hexagonal arrangement of the intestinal segments.

The absorbed dose to segment A is thus the result of self-dose and cross-dose from both walls and contents and can be written as:

$$D_{\text{total}} = D_{\text{self,wall}} + D_{\text{self,contents}} + D_{\text{cross,wall}} + D_{\text{cross,contents}} \quad \text{Eq. 2}$$

The self-absorbed dose and cross-organ dose were calculated for monoenergetic electrons with energies of 0.050, 0.10, 0.20, 0.50, 0.80, 1.0, 2.0, 5.0, 8.0, and 10 MeV and the radionuclides $^{99\text{m}}\text{Tc}$, ^{111}In , ^{131}I , ^{67}Ga , ^{90}Y , and ^{211}At including the complete decay scheme (17), assuming the activity distributed uniformly in the contents or the wall. For the radionuclides, the full β -particle

energy spectra were calculated by Fermi theory with the mean energy as the input. For electrons, the cross-dose was calculated only for the activity in the contents.

RESULTS

Electrons

The self-dose S values were calculated for monoenergetic electrons of 0.050, 0.10, 0.20, 0.50, 0.80, 1.0, 2.0, 5.0, 8.0, and 10 MeV, for activity uniformly distributed in the intestinal contents ($S_{\text{self,contents}}$) and in the intestinal wall ($S_{\text{self,wall}}$). These results are given in Table 2 for crypt cells for a wall thickness of 3 mm. For all energies, the self-dose from the wall exceeded that from the contents. For crypt cells and 0.050-MeV electrons, the ratio was about 10^5 , whereas for 10-MeV electrons it was 1.3.

Simulations of the cross-dose S values for crypt cells were also performed (Table 3). These S values were calculated assuming the electron source to be located in the intestinal contents ($S_{\text{cross,contents}}$). The self-dose contribution is higher than the cross-dose for electron energies between 0.5 and 5 MeV assuming the activity to be in the contents. For energies between 0.5 and 1 MeV, the self-dose contribution is 200–400 times higher than the cross-dose.

For low energies, 0.1 and 0.2 MeV, the cross-dose to the crypt cells was higher than the self-dose ($S_{\text{self,contents}}$) because of the contribution from bremsstrahlung. The continuous slowing-down approximation (CSDA) range for electron

TABLE 2
Self-Dose S Values for Crypt Cells for Electrons Assuming Activity Is Uniformly Distributed in Small Intestinal Wall (Thickness, 3 mm) and in Contents

Electron energy (MeV)	S value ($\text{mGy MBq}^{-1} \text{s}^{-1}$) at mucus thickness of			
	5 μm	50 μm	100 μm	200 μm
Wall				
0.05	$1.03 \cdot 10^{-5}$	$1.02 \cdot 10^{-5}$	$1.01 \cdot 10^{-5}$	$1.02 \cdot 10^{-5}$
0.1	$2.07 \cdot 10^{-5}$	$2.05 \cdot 10^{-5}$	$2.03 \cdot 10^{-5}$	$2.05 \cdot 10^{-5}$
0.2	$4.03 \cdot 10^{-5}$	$4.04 \cdot 10^{-5}$	$3.99 \cdot 10^{-5}$	$4.00 \cdot 10^{-5}$
0.5	$8.51 \cdot 10^{-5}$	$8.70 \cdot 10^{-5}$	$8.93 \cdot 10^{-5}$	$9.21 \cdot 10^{-5}$
0.8	$1.19 \cdot 10^{-4}$	$1.21 \cdot 10^{-4}$	$1.23 \cdot 10^{-4}$	$1.26 \cdot 10^{-4}$
1	$1.35 \cdot 10^{-4}$	$1.35 \cdot 10^{-4}$	$1.36 \cdot 10^{-4}$	$1.40 \cdot 10^{-4}$
2	$1.69 \cdot 10^{-4}$	$1.70 \cdot 10^{-4}$	$1.71 \cdot 10^{-4}$	$1.74 \cdot 10^{-4}$
5	$2.25 \cdot 10^{-4}$	$2.25 \cdot 10^{-4}$	$2.25 \cdot 10^{-4}$	$2.25 \cdot 10^{-4}$
8	$2.62 \cdot 10^{-4}$	$2.64 \cdot 10^{-4}$	$2.65 \cdot 10^{-4}$	$2.67 \cdot 10^{-4}$
10	$2.77 \cdot 10^{-4}$	$2.77 \cdot 10^{-4}$	$2.76 \cdot 10^{-4}$	$2.76 \cdot 10^{-4}$
Contents				
0.05	$9.10 \cdot 10^{-11}$	$8.87 \cdot 10^{-11}$	$8.83 \cdot 10^{-11}$	$8.67 \cdot 10^{-11}$
0.1	$3.67 \cdot 10^{-10}$	$3.50 \cdot 10^{-10}$	$3.13 \cdot 10^{-10}$	$3.04 \cdot 10^{-10}$
0.2	$1.35 \cdot 10^{-9}$	$1.40 \cdot 10^{-9}$	$1.38 \cdot 10^{-9}$	$1.24 \cdot 10^{-9}$
0.5	$7.98 \cdot 10^{-6}$	$7.03 \cdot 10^{-6}$	$6.15 \cdot 10^{-6}$	$4.60 \cdot 10^{-6}$
0.8	$2.20 \cdot 10^{-5}$	$2.09 \cdot 10^{-5}$	$1.98 \cdot 10^{-5}$	$1.76 \cdot 10^{-5}$
1	$3.12 \cdot 10^{-5}$	$2.99 \cdot 10^{-5}$	$2.97 \cdot 10^{-5}$	$2.64 \cdot 10^{-5}$
2	$7.49 \cdot 10^{-5}$	$7.34 \cdot 10^{-5}$	$7.19 \cdot 10^{-5}$	$6.91 \cdot 10^{-5}$
5	$1.74 \cdot 10^{-4}$	$1.72 \cdot 10^{-4}$	$1.70 \cdot 10^{-4}$	$1.67 \cdot 10^{-4}$
8	$2.06 \cdot 10^{-4}$	$2.05 \cdot 10^{-4}$	$2.03 \cdot 10^{-4}$	$2.00 \cdot 10^{-4}$
10	$2.13 \cdot 10^{-4}$	$2.12 \cdot 10^{-4}$	$2.10 \cdot 10^{-4}$	$2.07 \cdot 10^{-4}$

TABLE 3
Cross-Dose S Values for Electrons Assuming Uniform Distribution of Activity in Contents

Electron energy (MeV)	S value (mGy MBq ⁻¹ s ⁻¹) at mucus thickness of			
	5 μm	50 μm	100 μm	200 μm
0.1	6.37·10 ⁻¹⁰	5.61·10 ⁻¹⁰	5.68·10 ⁻¹⁰	6.04·10 ⁻¹⁰
0.2	2.58·10 ⁻⁹	2.64·10 ⁻⁹	2.61·10 ⁻⁹	2.61·10 ⁻⁹
0.5	2.04·10 ⁻⁸	1.97·10 ⁻⁸	1.98·10 ⁻⁸	2.01·10 ⁻⁸
0.8	5.20·10 ⁻⁸	5.16·10 ⁻⁸	5.18·10 ⁻⁸	5.12·10 ⁻⁸
1	7.34·10 ⁻⁸	7.36·10 ⁻⁸	7.37·10 ⁻⁸	7.40·10 ⁻⁸
2	4.16·10 ⁻⁶	4.31·10 ⁻⁶	4.46·10 ⁻⁶	4.77·10 ⁻⁶
5	1.06·10 ⁻⁴	1.04·10 ⁻⁴	1.05·10 ⁻⁴	1.06·10 ⁻⁴
8	2.56·10 ⁻⁴	2.53·10 ⁻⁴	2.54·10 ⁻⁴	2.54·10 ⁻⁴
10	3.70·10 ⁻⁴	3.67·10 ⁻⁴	3.67·10 ⁻⁴	3.67·10 ⁻⁴

energies of 0.1 and 0.2 MeV are 0.14 and 0.45 mm, respectively (18). The cross-dose also exceeded the self-dose for high energies, 8 and 10 MeV. For 10-MeV electrons, the S values for the crypt cells from the intestinal loops nearby ($S_{cross,contents}$) were almost twice as high as the self-dose from the contents ($S_{self,contents}$). The CSDA range for 8-MeV electrons is 4.0 cm and for 10-MeV electrons it is 5.0 cm (18).

Radionuclides

Self-dose S values for the radionuclides ^{99m}Tc, ¹¹¹In, ¹³¹I, ⁶⁷Ga, ⁹⁰Y, and ²¹¹At are presented in Table 4 with data for both electrons and photons (except for the pure β-emitter ⁹⁰Y). In Table 5, cross-dose S values are given for these same radionuclides. Because the variation with mucus thickness is less than ±1% for all of these radionuclides except for ⁹⁰Y, data for a mucus thickness of 5 μm are given in Table 5. For ⁹⁰Y, the S value for the 200-μm mucus thickness is 17% higher than that for the 5-μm thickness. Data for ²¹¹At for α-particles, electrons, and photons are presented in Table 6. The energy of the α-particles was considered to be locally absorbed.

For the radionuclides studied, the self-dose S value assuming the activity to be distributed in the contents ($S_{self,contents}$) is up to a factor 5 less than that from the cross-dose ($S_{cross,contents}$). The self-dose from wall activity ($S_{self,wall}$) is up to 7 times higher than the cross-dose ($S_{cross,wall}$). The cross-dose for electrons ($S_{cross,wall}$) from the radionuclides in the wall is negligible, even for ⁹⁰Y with a maximum β⁻-particle energy of 2.282 MeV and a CSDA range of 1.1 cm (18). In Figures 2A, 2B, and 2C, the S values for ^{99m}Tc, ¹³¹I, and ⁹⁰Y, respectively, are

TABLE 4
Self-Dose S Values for Different Radionuclides Assuming Activity Is Uniformly Distributed in Small Intestinal Wall (Thickness, 3 mm) and in Contents

Mucus thickness (μm)		S value (mGy MBq ⁻¹ s ⁻¹)					
		^{99m} Tc	¹¹¹ In	¹³¹ I	⁶⁷ Ga	⁹⁰ Y	²¹¹ At*
Wall							
5	Electron	3.23·10 ⁻⁶	7.03·10 ⁻⁶	3.73·10 ⁻⁵	6.97·10 ⁻⁶	1.17·10 ⁻⁴	1.18·10 ⁻⁶
	Photon	5.92·10 ⁻⁷	2.48·10 ⁻⁶	1.83·10 ⁻⁶	1.47·10 ⁻⁶		3.81·10 ⁻⁷
	Total	3.82·10 ⁻⁶	9.52·10 ⁻⁶	3.92·10 ⁻⁵	8.43·10 ⁻⁶		1.57·10 ⁻⁶
50	Electron	3.23·10 ⁻⁶	6.98·10 ⁻⁶	3.73·10 ⁻⁵	6.98·10 ⁻⁶	1.18·10 ⁻⁴	1.19·10 ⁻⁶
	Photon	5.85·10 ⁻⁷	2.49·10 ⁻⁶	1.84·10 ⁻⁶	1.49·10 ⁻⁶		3.85·10 ⁻⁷
	Total	3.82·10 ⁻⁶	9.47·10 ⁻⁶	3.91·10 ⁻⁵	8.47·10 ⁻⁶		1.57·10 ⁻⁶
100	Electron	3.25·10 ⁻⁶	6.95·10 ⁻⁶	3.75·10 ⁻⁵	7.02·10 ⁻⁶	1.20·10 ⁻⁴	1.19·10 ⁻⁶
	Photon	6.01·10 ⁻⁷	2.47·10 ⁻⁶	1.85·10 ⁻⁶	1.48·10 ⁻⁶		3.88·10 ⁻⁷
	Total	3.85·10 ⁻⁶	9.42·10 ⁻⁶	3.93·10 ⁻⁵	8.50·10 ⁻⁶		1.57·10 ⁻⁶
200	Electron	3.22·10 ⁻⁶	6.96·10 ⁻⁶	3.80·10 ⁻⁵	7.03·10 ⁻⁶	1.22·10 ⁻⁴	1.18·10 ⁻⁶
	Photon	6.06·10 ⁻⁷	2.47·10 ⁻⁶	1.83·10 ⁻⁶	1.46·10 ⁻⁶		3.99·10 ⁻⁷
	Total	3.82·10 ⁻⁶	9.44·10 ⁻⁶	3.99·10 ⁻⁵	8.50·10 ⁻⁶		1.58·10 ⁻⁶
Contents							
5	Electron	6.70·10 ⁻¹¹	2.58·10 ⁻¹⁰	6.42·10 ⁻⁷	2.83·10 ⁻¹⁰	2.95·10 ⁻⁵	1.55·10 ⁻⁹
	Photon	4.40·10 ⁻⁷	1.79·10 ⁻⁶	1.42·10 ⁻⁶	6.13·10 ⁻⁷		1.89·10 ⁻⁷
	Total	4.40·10 ⁻⁷	1.79·10 ⁻⁶	2.06·10 ⁻⁶	6.14·10 ⁻⁷		1.91·10 ⁻⁷
50	Electron	6.47·10 ⁻¹¹	1.76·10 ⁻¹⁰	5.09·10 ⁻⁷	1.83·10 ⁻¹⁰	2.76·10 ⁻⁵	1.46·10 ⁻⁹
	Photon	4.37·10 ⁻⁷	1.77·10 ⁻⁶	1.40·10 ⁻⁶	6.06·10 ⁻⁷		1.88·10 ⁻⁷
	Total	4.37·10 ⁻⁷	1.77·10 ⁻⁶	1.91·10 ⁻⁶	6.07·10 ⁻⁷		1.89·10 ⁻⁷
100	Electron	6.33·10 ⁻¹¹	1.58·10 ⁻¹⁰	4.01·10 ⁻⁷	1.25·10 ⁻¹⁰	2.65·10 ⁻⁵	1.36·10 ⁻⁹
	Photon	4.36·10 ⁻⁷	1.75·10 ⁻⁶	1.38·10 ⁻⁶	5.92·10 ⁻⁷		1.83·10 ⁻⁷
	Total	4.36·10 ⁻⁷	1.75·10 ⁻⁶	1.79·10 ⁻⁶	5.92·10 ⁻⁷		1.84·10 ⁻⁷
200	Electron	5.93·10 ⁻¹¹	1.55·10 ⁻¹⁰	2.45·10 ⁻⁷	8.73·10 ⁻¹¹	2.47·10 ⁻⁵	1.11·10 ⁻⁹
	Photon	4.26·10 ⁻⁷	1.72·10 ⁻⁶	1.37·10 ⁻⁶	5.71·10 ⁻⁷		1.77·10 ⁻⁷
	Total	4.26·10 ⁻⁷	1.72·10 ⁻⁶	1.61·10 ⁻⁶	5.71·10 ⁻⁷		1.78·10 ⁻⁷

*α-Particles excluded.

TABLE 5

Cross-Dose S Values for Crypt Cells for Different Radionuclides (Wall Thickness, 3 mm; Mucus Thickness, 5 μm)

Radionuclide	S value (mGy MBq ⁻¹ s ⁻¹)	
	Activity in contents	Activity in wall
^{99m} Tc	1.97·10 ⁻⁶	2.26·10 ⁻⁶
¹¹¹ In	6.45·10 ⁻⁶	7.32·10 ⁻⁶
¹³¹ I	5.74·10 ⁻⁶	6.29·10 ⁻⁶
⁶⁷ Ga	2.35·10 ⁻⁶	2.64·10 ⁻⁶
⁹⁰ Y	2.85·10 ⁻⁷	N/A
²¹¹ At	6.85·10 ⁻⁷	8.00·10 ⁻⁷

N/A = not applicable.

given for different source locations; the contributions from electrons and photons are presented separately. Figures 2A–2C show that the dominating S value is the self-dose from the activity in the wall ($S_{self,wall}$) for the 3-mm wall thickness.

Mucus Thickness

When the activity is distributed in the intestinal contents, the mucus thickness is of importance only for the dose from low electron energies (0.050–0.20 MeV). The S values for the villi are up to >800 times higher for the thinnest mucus layer (5 μm) than for the thickest mucus layer (200 μm). For the electron energies 0.50–10 MeV, the ratio is ≤ 1.5 .

The mucus thickness had less influence on the S value for the crypt cells than for the villi, both for the monoenergetic electrons and for the radionuclides simulated. With the activity in the contents, the S value ratios (5- μm mucus thickness/200- μm mucus thickness) for crypt cells were <1.8 for electrons and <3.3 for the electrons for the radionuclides.

For villi, the electron contribution from the radionuclides depends on the thickness of the mucus layer. ¹³¹I, ⁹⁰Y, and ²¹¹At showed a variation of the S value ratio ($S_{5\mu\text{m}}/S_{200\mu\text{m}}$) of

TABLE 6

S Values for ²¹¹At Assuming Activity Is Uniformly Distributed in Intestinal Wall (Wall Thickness, 3 mm; Mucus Thickness, 5 μm)

Type of radiation	Energy (MeV)	Dose	S value (mGy MBq ⁻¹ s ⁻¹)
α -Particles	5.867	Self-dose*	4.95·10 ⁻⁴
Recoil particles	0.113	Self-dose	9.57·10 ⁻⁶
Electrons	$\leq 0.670^\dagger$	Self-dose [‡]	1.18·10 ⁻⁶
Photons	$\leq 0.687^\dagger$	Self-dose [‡]	3.81·10 ⁻⁷
Photons	$\leq 0.687^\dagger$	Cross-dose [‡]	8.00·10 ⁻⁷

*Energy of α -particles is considered to be locally absorbed.
[†]Numerous energies.
[‡]Dose to crypt cells.

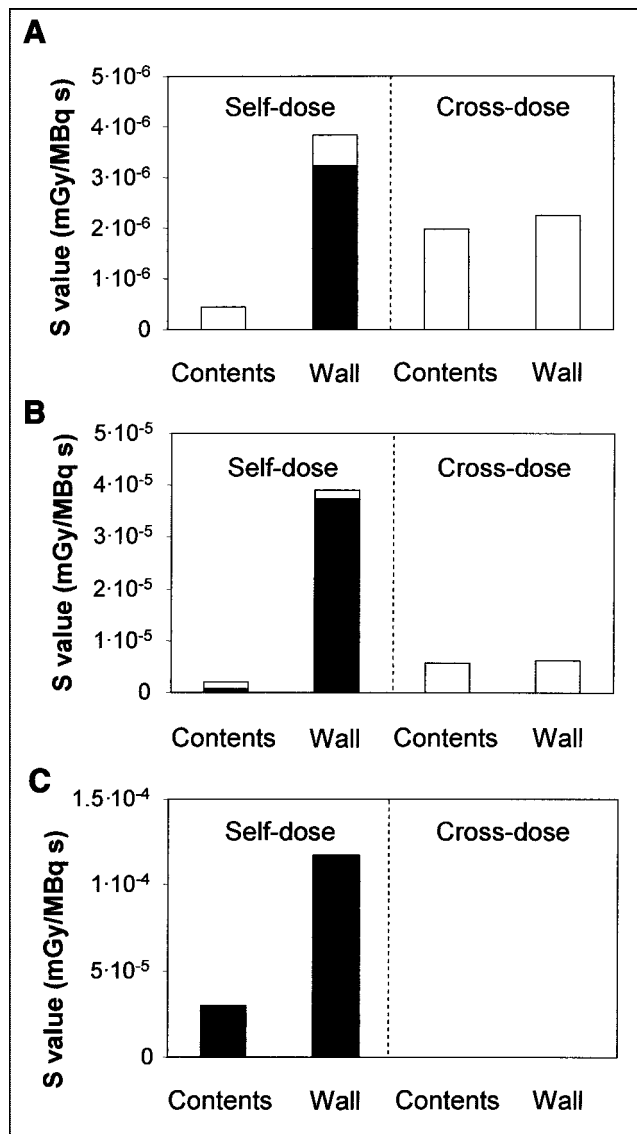


FIGURE 2. Crypt cell S values for radionuclide located in intestinal contents or wall (3 mm) for ^{99m}Tc (A), ¹³¹I (B), and ⁹⁰Y (C). Contributions from electrons (■) and from photons (□) are illustrated for each absorbed dose component.

<2.5. For ^{99m}Tc, the S value was >800 times greater for a mucus thickness of 5 μm than for a mucus thickness of 200 μm . For ⁶⁷Ga and ¹¹¹In, the corresponding values were about 50 and 10 times, respectively (Fig. 3).

Wall Thickness

The variation in the self-dose S values with intestinal wall thickness (ratio for 3- to 6-mm wall thickness) is 2.1–2.3 for electron energies in the range 0.05–1.0 MeV and 1.3–1.6 for the higher energies, 2.0–10 MeV. A higher S value for the thinner intestinal wall is explained by the higher activity concentration because the S value is calculated per megabecquerel of the radionuclides and per 10⁶ electrons, respectively. The radionuclides show the same variation with wall size for electrons, 2.2, because of low electron energies. A smaller variation, 1.9, is seen for ⁹⁰Y.

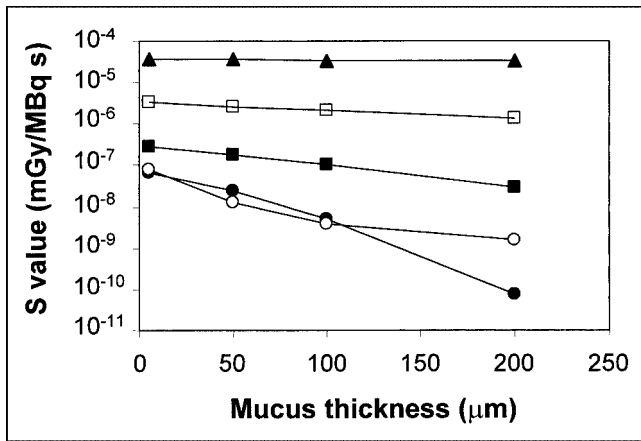


FIGURE 3. Variation in self-dose S values for villi for electrons from different radionuclides located in intestinal contents as function of mucus thickness. ●, ^{99m}Tc ; ■, ^{111}In ; ○, ^{67}Ga ; □, ^{131}I ; ▲, ^{90}Y .

For low-energy, monoenergetic electrons, 0.05–0.10 MeV, the S value for the activity in the intestinal wall ($S_{\text{self,wall}}$) is 50–100,000 times higher than that for the contents ($S_{\text{self,contents}}$), depending on the thickness of the mucus layer (Fig. 4). A corresponding comparison for the radionuclides shows a ratio of the same magnitude for the electron contribution. The photon S values are 1.3–2.5 times higher for the wall self-dose ($S_{\text{self,wall}}$) than the contents self-dose ($S_{\text{self,contents}}$). This results in total S values about 5–25 times higher for the activity in the wall (thickness, 3 mm) than in the contents. S values for ^{211}At are presented in Table 6 assuming the activity is distributed uniformly in the intestinal wall (thickness, 3 mm). The dominating dose contribution is from the α -particle and recoil of the residual nucleus.

DISCUSSION

In this study, a new model for internal dosimetry of the small intestine has been developed, making more detailed and accurate dosimetry possible. Because of individual biologic variation and differences in the methods of data collection, there is an uncertainty in all data used in an anatomic model.

Several values are given in the literature for the diameter of the small intestine, ranging from 1.5 to 6 cm (3,9,12–14,19). The diameter varies along the intestine from the duodenum to the ileum and because of intestinal movement. In this study, an average inner diameter of 2.5 cm was used for the small intestine.

The reported length of the small intestine in vivo is 3 m, with a variation between 2 and 4 m (9,12–15,19). Various values of the small intestinal wall thickness are also reported in the literature. The ICRP (14) gives wall thicknesses between 2 and 6 mm. The National Council on Radiation Protection and Measurements (NCRP) (15) gives a value of 3 mm and Eve (9) gives a value of 2–3 mm. In

the model by Stubbs et al. (3), a wall thickness of 5 mm was used, whereas Poston et al. (4) used a value of 7.54 mm. Reported anatomic data indicate that there is some variation along the small intestine, and there will almost certainly be differences between individuals. In the model used in this investigation, 2 different values of the wall thickness were used, 3 and 6 mm.

The location of the most radiation-sensitive cells is important. In this study a villi length of 500 μm and a crypt depth of 150 μm were used in the simulations. In the literature, however, large variations in villi lengths and crypt depths can be found. Villi lengths between 300 μm and 1.5 mm are given (3,9,12,14,15,19,20) and 140–500 μm is given for crypt depths (3,9,15).

Most intestinal models for absorbed dose calculations do not take the mucus thickness into account. In the study by Stubbs et al. (3), however, a value of 200 μm was used. We have chosen thicknesses between 5 and 200 μm , based on information regarding the thickness of the mucus layer on living human tissues, obtained from an experienced pathologist.

In earlier studies involving a cylindrical model (3,4), the cross-dose was not calculated. With regard to the radionuclides studied, the magnitude of the S value largely depends on the activity distribution in the wall and the contents. This also affects the fraction of the absorbed dose arising from the self-dose and cross-dose.

Table 7 compares S values for the radionuclides with S values given by other authors (2,3,21–24). The S values of Stubbs et al. (3) were calculated assuming an activity of 1 Bq/10 cm of intestine. Their data were correlated with the total cumulated activity in the same way as our data. The data of Stubbs et al. (3) represent the S values at a distance about 550 μm from the mucus–wall interface, where it was assumed that the sensitive crypt cells are located.

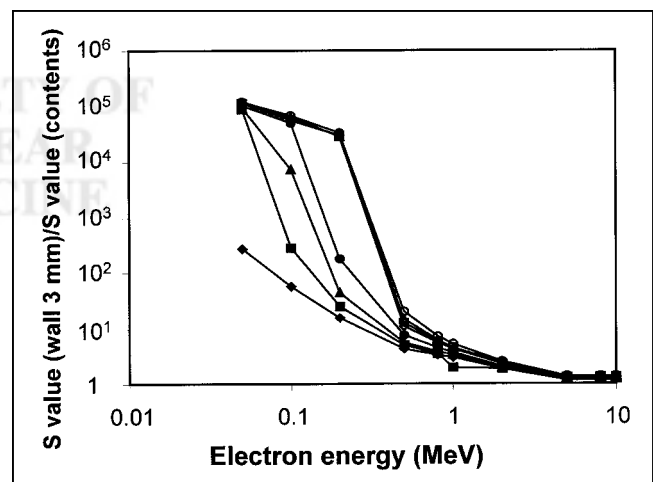


FIGURE 4. Ratio of S values for 3-mm wall as source tissue and contents as source for different electron energies for villi (filled symbols) and crypt cells (open symbols) and different mucus thicknesses. ◆, ◇, 5 μm ; ■, □, 50 μm ; ▲, △, 100 μm ; ●, ○, 200 μm .

TABLE 7
Total S Values for Small Intestinal Wall from Different Radionuclides

Reference	Source tissue	Target tissue	Dose	S value (mGy MBq ⁻¹ s ⁻¹)				
				^{99m} Tc	¹¹¹ In	¹³¹ I	⁶⁷ Ga	⁹⁰ Y
ICRP (21–23)*	Contents	SI wall	Total	5.6·10 ⁻⁶	1.5·10 ⁻⁵	4.5·10 ⁻⁵	1.0·10 ⁻⁵	1.9·10 ⁻⁴
MIRD (2)	Contents	SI wall	Total	5.9·10 ⁻⁶	1.6·10 ⁻⁵	4.5·10 ⁻⁵	1.1·10 ⁻⁵	1.9·10 ⁻⁴
MIRDOSE 3 (24)	Contents	SI wall	Total	4.4·10 ⁻⁶	1.1·10 ⁻⁵	4.0·10 ⁻⁵	8.9·10 ⁻⁶	1.8·10 ⁻⁴
Stubbs et al. (3) [†]	Contents	Crypt cells	Self-dose	4·10 ⁻⁷	N/A	2·10 ⁻⁶	N/A	4·10 ⁻⁵
This work [†]	Contents	Crypt cells	Total	2.4·10 ⁻⁶	8.2·10 ⁻⁶	7.3·10 ⁻⁶	2.9·10 ⁻⁶	2.5·10 ⁻⁵
This work [†]	Wall	Crypt cells	Total	6.1·10 ⁻⁶	1.8·10 ⁻⁵	4.6·10 ⁻⁵	1.1·10 ⁻⁵	1.2·10 ⁻⁴

*Recalculated from specific effective energy values.
[†]S values given for activity in total small intestine.
SI = small intestinal; N/A = not applicable.
S values are given for mucus thickness of 200 μm (3; this work) and wall thickness of 3 mm (this work).

We found good agreement when comparing our self-dose S values to villi and crypt cells, assuming the activity is in the contents ($S_{self,contents}$), with the data of Stubbs. However, the data presented by the ICRP (21–23), MIRD (2), and MIRDOSE3 (24) disagree with our data by factors in a range of 7–28.

In Table 7 the total S value is given for crypt cells assuming the activity is located in either the contents or the wall. When comparing the total S values with those given by MIRD (2) and the ICRP (21–23) (Table 7), we found that they are of the same order of magnitude. Because the assumed biodistribution is not necessarily the actual one, our separate S values should be used when data exist separately for intestinal wall and contents.

In a further development, other source locations could be applied in the model. The mucosal region, or parts of it (e.g., villi or crypt cells), can be used in the simulations as the source region and corresponding S values can be calculated. In this study, a uniform activity distribution in the intestinal wall was used; however, data from autoradiographic studies can be included to further refine the model for specific radiopharmaceuticals.

The distance to the most sensitive cells in the intestinal mucosa was assumed to be constant in this study. However, the small intestine is not static, because of peristaltic movements, and thus the distance to the crypt cells from the activity in the contents will vary. The total thickness can be the sum of the thickness of the mucus layer, the villi length, and the crypt depth. However, when the intestine is moving, the activity can be located in the mucus directly above the crypts. The dosimetric data presented in this study could easily be implemented in a dynamic model for the intestine.

To make full use of this new detailed model, the activity distributions in the intestinal wall and contents are required. Also, the biokinetics of the radiopharmaceutical must be known. To obtain a more accurate value of the absorbed dose, both animal data, giving detailed information concerning the activity distribution within the small intestinal wall, and complementary human data should be obtained. This

would allow even more detailed calculations of the absorbed dose to the radiation-sensitive cells in the intestinal wall.

CONCLUSION

A small intestinal model was developed for calculation of the absorbed dose to the radiation-sensitive crypt cells. The activity distribution in the intestinal wall and contents is taken into consideration in this model, which was not the case in earlier models. Not only the self-dose but also the contribution from the nearby intestinal loops—that is, the cross-dose—can be calculated in this model.

ACKNOWLEDGMENTS

This study was supported in part by the Swedish Cancer Society, the Swedish Medical Research Council, Gunnar Nilsson's Cancer Foundation, and Berta Kamprad's Foundation for Cancer Treatment.

REFERENCES

- International Commission on Radiological Protection. *Limits for Intakes of Radionuclides by Workers*. ICRP Publication 30: Part 1. New York, NY: Pergamon Press; 1979.
- Snyder WS, Ford MR, Warner GG, Watson SB. "S," *Absorbed Dose per Unit Cumulated Activity for Selected Radionuclides and Organs*. MIRD Pamphlet No. 11. New York, NY: Society of Nuclear Medicine; 1975.
- Stubbs JB, Evans JF, Stabin MG. Radiation absorbed doses to the walls of hollow organs. *J Nucl Med*. 1998;39:1989–1995.
- Poston JW Jr, Kodimer KA, Bolch WE, Poston JW Sr. A revised model for the calculation of absorbed energy in the gastrointestinal tract. *Health Phys*. 1996; 71:307–314.
- Jönsson BA, Strand SE, Larsson BS. A quantitative autoradiographic study of the heterogeneous activity distribution of different indium-111-labeled radiopharmaceuticals in rat tissues. *J Nucl Med*. 1992;33:1825–1833.
- Lathrop KA, Lathrop DA, Harper PV. Propriety of the ICRP model for estimation of radiation dose to the gastrointestinal tract from intravenously administered ²⁰¹TlCl. In: S-Stelson AT, Stabin MG, Sparks RB, eds. *Proceedings of the Sixth International Radiopharmaceutical Dosimetry Symposium*. Oak Ridge, TN: Oak Ridge Associated Universities; 1999:479–486.
- Som P, Matsui K, Atkins HL, et al. Microautoradiographic studies on the cellular localization of radiothallium. *Nuklearmedizin*. 1978;17:266–296.
- Loevinger R, Berman M. *A Revised Schema for Calculating the Absorbed Dose from Biologically Distributed Radionuclides*. MIRD Pamphlet No. 1 (revised). New York, NY: Society of Nuclear Medicine; 1976.

9. Eve IS. A review of the physiology of the gastrointestinal tract in relation to radiation doses from radioactive materials. *Health Phys.* 1966;12:131–161.
10. Snyder WS, Ford MR, Warner GG. *Estimates of Specific Absorbed Fractions for Photon Sources Uniformly Distributed in Various Organs of a Heterogeneous Phantom.* MIRD Pamphlet No. 5 (revised). New York, NY: Society of Nuclear Medicine; 1978.
11. Stabin MG, Watson EE, Cristy M, et al. *Mathematical Models and Specific Absorbed Fractions of Photon Energy in the Nonpregnant Adult Female and at the End of Each Trimester of Pregnancy.* ORNL/TM-12907. Oak Ridge, TN: Oak Ridge National Laboratory; 1995.
12. Tortora GJ, Grabowski SR. *Principles of Anatomy and Physiology.* 8th ed. New York, NY: HarperCollins; 1996.
13. Kararli TT. Comparison of the gastrointestinal anatomy, physiology and biochemistry of humans and commonly used laboratory animals. *Biopharm Drug Dispos.* 1995;16:351–380.
14. International Commission on Radiological Protection. *Report of the Task Group on Reference Man.* ICRP Publication 23. New York, NY: Pergamon Press; 1975.
15. National Council on Radiation Protection and Measurements. *Biological Effects and Exposure Limits for "Hot Particles."* NCRP Report No. 130. Bethesda, MD: National Council on Radiation Protection and Measurements; 1999.
16. Bielajew AF, Rogers DWO. PRESTA: the parameter reduced electron-step algorithm for electron Monte Carlo transport. *Nucl Instrum Methods B.* 1987;18:165–181.
17. Weber DA, Eckerman KF, Dillman LT, Ryman JC. *MIRD: Radionuclide Data and Decay Schemes.* New York, NY: The Society of Nuclear Medicine; 1989.
18. International Commission on Radiation Units and Measurements. *Stopping Powers for Electrons and Positrons.* ICRP Publication 37. Bethesda, MD: International Commission on Radiation Units and Measurements; 1984.
19. Marieb EN. *Human Anatomy and Physiology.* 2nd ed. Redwood City, CA: Benjamin/Cummings Publishing; 1992.
20. Shiner M. Anatomy of the small intestine. In: Haubrich WS, Schaffner F, Berk JE, eds. *Bockus Gastroenterology.* 5th ed. Philadelphia, PA: W.B. Saunders; 1995:885–898.
21. International Commission on Radiological Protection. *Limits for Intakes of Radionuclides by Workers.* ICRP Publication 30: Supplement to Part 1. New York, NY: Pergamon Press; 1979.
22. International Commission on Radiological Protection. *Limits for Intakes of Radionuclides by Workers.* ICRP Publication 30: Supplement to Part 2. New York, NY: Pergamon Press; 1979.
23. International Commission on Radiological Protection. *Limits for Intakes of Radionuclides by Workers.* ICRP Publication 30: Supplement A to Part 3. New York, NY: Pergamon Press; 1979.
24. Stabin M. MIRDOSE: personal computer software for internal assessment in nuclear medicine. *J Nucl Med.* 1996;37:538–546.

